

Chapter 1

A Hybrid-DE for Automatic Retinal Image-Based Blood Vessel Segmentation

Colin Paul Joy¹, Kamlesh Mistry², Gobind Pillai¹, Li Zhang³

¹*School of Computing,, Teesside University, Middlesbrough TS1 3BX, UK*

²*Computer and Information Sciences, Northumbria University, NE1 8ST, UK*

³*Department of Computer Science, Royal Holloway, University of London, UK*

Abstract

The retinal vein segmentation assumes a significant job in programmed or PC helped diagnosis of retinopathy. Manual vein segmentation is very tedious and requires a lot of subject specific information. Also, the veins are just a couple of pixels wide and spread across the whole fundus image. This further impedes the ongoing frameworks from mechanizing the retinal vein segmentation productively. In this paper, we propose a novel Hybrid Differential Evolution (DE) to complete programmed retinal vein segmentation. The proposed DE starts by generating three dynamic sets of populations focusing on thick veins, thin veins and non-veins. It also employs a non-replaceable memory concept to store all the three initial population members. Then in order to further balance the local and global exploration a micro firefly optimization algorithm with three mutations techniques is embedded in the core of DE. Various classifiers, for example, Neural Networks (NN), Support vector machines (SVM), NN and SVM based ensemble are utilized to additionally evaluate the performance of the segmentation system. The proposed system is assessed on the openly accessible DRIVE, STARE and HRF retinal image datasets and it outflanked cutting edge strategies

with a high normal precision of 98.5% alongside high affectability and explicitness.

1. Introduction

Retinal vein segmentation and portrayal of basic properties of veins like length, width, convolution and repercussion design are utilized for retinal determination, investigation, treatment, and evaluation of diverse visual ailment like diabetes, hypertension and so forth. The changes in retinal veins can aid the medical diagnosis of diseases such as diabetic retinopathy, glaucoma, retinal artery occlusion, branch vein occlusion, central retinal vein occlusion, diabetes etc. In current situation, fast development of diabetes is one of the major difficulties of wellbeing assurance. If it is not treated in time, then it may lead to visual deficiency in individuals before middle age that causes vision misfortune. In order to conduct an efficient and accurate diabetic retinopathy, a system is required that can segment retinal vein from retinal images and analyse it. Medical group people acknowledge that manual vessel segmentation can provide accurate segmentation but at the same time significant amount of time and domain knowledge is required. This urges for a need of an automated retinal vein segmentation system. In biomedical, robotized retinal vein segmentation are becoming progressively popular for detecting retinal pathologies. Retinal Veins can be seen in different thickness levels, thick veins are easily identifiable but segmenting the thin veins is very tedious and challenging for both automated and manual systems. Over the time many researchers have worked on automated retinal vein segmentation methods such as matched filter, multiscale strategy, vessel tracking, and pattern classification-based methodology. In the present situation matched filter is the most popular method for the retinal vein segmentation due to its segmentation accuracy. In order to address the above-mentioned challenges and constraints, this paper proposes a novel variant of DE to segment the retinal vein images. The main contributions of the proposed system are pointed below:

1. A novel DE variant is proposed for retinal vein segmentation, which employs three population approach to identify each category of vein i.e. Thick veins, thin veins and non-vein areas.
2. Micro-FireFly Algorithm (mFA) is embedded with the multi-population DE algorithm, in order to mitigate the premature convergence and local optimum problems of conventional DE.
3. The proposed DE variant also applies the diversity maintenance strategy of micro-Genetic Algorithm (mGA) to keep all the original populations in a non-replaceable memory, which remains intact during the lifetime of the algorithm, in order to reduce the probability of premature convergence.
4. Our proposed system is evaluated with DRIVE, STARE and HRF datasets and is also compared with other existing methods reported in the literature.

This paper explores the discrimination capabilities in the texture of fundus to differentiate between healthy and un-healthy images, where the focus is to examine the performance of an extended variant of differential evolution (DE) to carry out automatic retinal blood vessel segmentation. An overall system architecture diagram is presented in Fig. 1. The rest of the paper is structured as follows: Section 2 focuses on related work, Section 3 focuses on retinal vein segmentation system including the details on proposed DE variant, the Section 4 focuses on Evaluation of the proposed system and finally the Section 5 concludes the work while addressing future directions.

2. Related Work

The authors [1] proposed an automated retinal blood vessel segmentation using artificial bee colony optimization and fuzzy c-means clustering. In their work artificial bee colony optimization is used as global search method to find cluster centers of the fuzzy c-means objective function. In order to localize small vessels with a different fitness function, a pattern search approach was used for optimization. Hassan et al. [2] used blood vessel segmentation approach to extract the vasculature on retinal fundus images. Their work involved Particle Swarm Optimization (PSO) to

determine the $n-1$ optimal n -level thresholds on retinal fundus images. Their work was tested on the DRIVE datasets and its efficiency compared with alternative methods. The approach proposed by Sreejini and Govindan [3] made use of improved noise suppression features of multiscale Gaussian matched filter. The parameter values of the filter were obtained through particle swarm optimization and hence the accuracy of retina vessel segmentation was improved. Arnay et al. [4] worked on the optic cup segmentation in retinal fundus images using Ant Colony Optimization approach. In their approach, artificial agents produced solutions through a heuristic that used the intensity gradient of the optic disc area and the curvature of the vessels. The exploration capabilities of the agents were limited on their own, but by sharing the experience of the entire colony, they obtained accurate cup segmentations, even in images with a weak or non-obvious pallor. In the paper by Wang et al. [5], a supervised method involving two superior classifiers namely Convolutional Neural Network (CNN) and Random Forest (RF) was used to deal with retinal blood vessel segmentation. The CNN was first used as a trainable hierarchical feature extractor and then ensemble RFs worked as a trainable classifier. Their approach combined the merits of feature learning and traditional classifier and was able to automatically learn features from the raw images and predict the patterns. Morales et al. [6] worked on differentiating between the texture of fundus images in case of pathological and healthy images. The authors used LBP as a texture descriptor tool for retinal images and compared their work with other descriptors such as LBP filtering and local phase quantization. Hatami and Goldbaum [7] proposed a novel LBP method and showed that it was robust against low contrast and low-quality fundus images, and it helped in image classification by including additional AV texture and shape information. Fraz et al. [8] presented a survey of the blood vessel segmentation methods in two-dimensional, fundus camera acquired retinal images. Their paper has details about review, analysis and classification of the retinal vessel extraction algorithms and methodologies along with highlights of the key points and the performance measures.

Staal et al. [9] proposed ridge-based vessel segmentation method in coloured images of the retina. The system extracted the image ridges based on the vessel centerlines. The ridges were then used to compose primitive line elements which helped an image to be partitioned into patches. Each image pixel was then assigned to the closest line element, which formed a local coordinate frame for its corresponding patch. The feature vector thereby computed for every pixel utilized the properties of the patches and the line elements. Sequential forward feature selection was used for feature selection and kappaNN-classifier to classify the feature vectors. Accuracy of 0.944 versus 0.947 for a second observer was reported in their work.

Marin et al. [10] used a new supervised method for detection of blood vessel in digital retinal images. They used a neural network (NN) for pixel classification and computed a 7-D vector composed of grey-level and moment invariants-based features for pixel representation. The authors showed that their algorithm was effective and robust for automated screening and detection in patients with early diabetic retinopathy.

In the work by You et al. [11], novel extracting of the retinal vessels based on radial projection and semi-supervised method is presented. Any segmentation method would need to consider two different processes to detect different types of vessels namely thin and wide vessels. The radial projection method locates the vessel centerlines and the steerable complex wavelet provides better capability of enhancing vessels under different scales. The feature vector then represents the vessel pixel line strength. The major structures of vessels are then identified using semi-supervised self-training and the union of the thin and wide vessels produces the final image segmentation.

Budai et al. [12] showed a method which reduced calculation time, obtained high accuracy, and increased the sensitivity as compared to the original Frangi method. With improvements in technology, the quality and resolution of fundus images are rapidly increasing, hence the segmentation methods would need to tackle the new challenges of high resolutions. The results in their work, showed an average accuracy over 94% with the benefit of low computational burden. Hannink et al. [13] proposed a new method using scale–orientation scores that performed

much better at enhancing vessels throughout crossings and bifurcations than the multi-scale Frangi filter which is an established tool in retinal vascular imaging. The authors presented results using both methods on a public dataset.

Chakraborti et al. [14] used self-adaptive matched filter method for the blood vessel detection in the retinal fundus images. They used orientation histogram and presented a new combination of the vesselness filter giving high sensitivity and the matched filter giving high specificity.

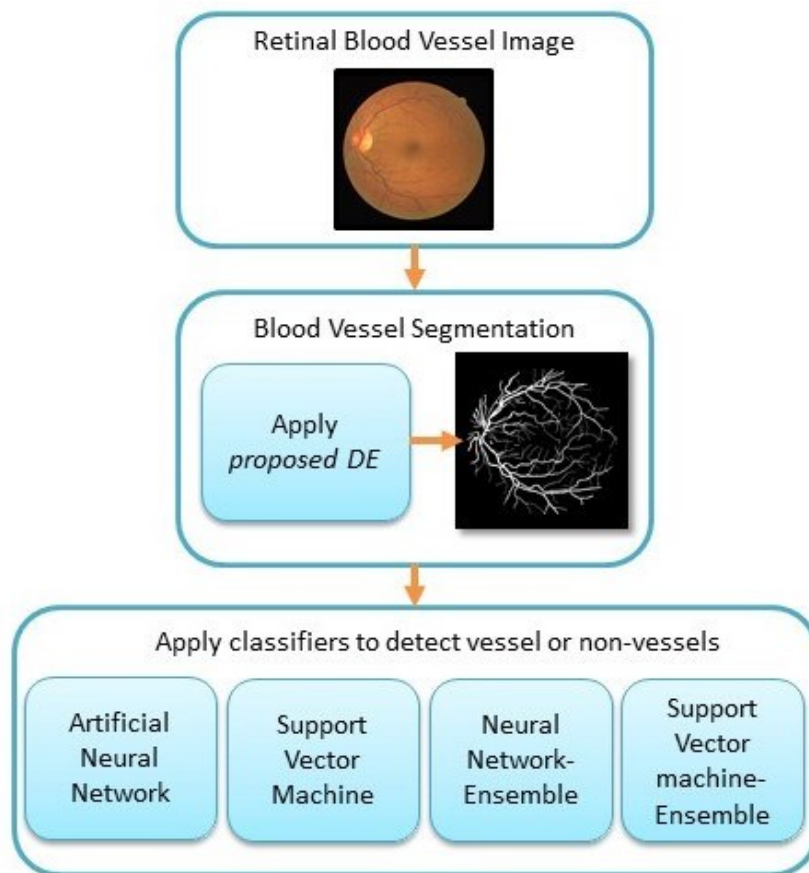


Figure 1: System architecture of the proposed system

3. Proposed System

In this section, we introduce the proposed retinal image analysis system. The overall system consists of two key steps, i.e. A *hvnLBP*-based feature extraction and proposed DE based segmentation. Each step is introduced in detail in the following sub-sections.

3.1 The horizontal vertical neighborhood LBP

Ojala et al. [15] proposed the conventional LBP which thresholds each of the 3x3 neighboring pixels with a center pixel value. The conventional LBP was further extended to use various numbers of circular neighboring pixels. The LBP operator $LBP_{p,r}$ can produce 2^p different binary patterns, where p denotes the number of neighborhood pixels and r denotes the radius of the circular pattern. The equation for calculating the $LBP_{p,r}$ operator can be given as follows:

$$LBP_{p,r} = \sum_{p=0}^{p-1} S(g_p - g_c) 2^p, S(x) = \begin{cases} 1 & \text{if } x \geq 0 \\ 0 & \text{otherwise} \end{cases} \quad (1)$$

where g_p denotes the neighborhood pixel at location p and g_c is the center pixel. The important information such as edges, corners, spot and flat area can be detected using the LBP. The conventional LBP is robust to illumination and scaling variations but fails to deal with rotation variations. Whereas, the gradient images contain enhanced edge information and are more stable than raw pixel intensities, which can benefit to deal with rotation and illumination variations.

In order to improve the feature extraction quality in terms of low contrast ration, Mistry et al. [16] proposed horizontal vertical neighborhood LBP (*hvnLBP*). The *hvnLBP* operator can be calculated by using the following equation:

$$hvnLBP_{p,r} = \{S(\max(p_0, p_1, p_2)), S(\max(p_7, p_3)), \\ S(\max(p_6, p_5, p_4)), S(\max(p_0, p_7, p_6)), \\ S(\max(p_1, p_5)), S(\max(p_2, p_3, p_4))\} \quad (2)$$

Where p_i denotes the pixel intensity of neighborhood pixels at the i^{th} location, r is the radius, and S denotes the comparison operation, as follows.

$$S(\max(p_j, p_k, p_m)) = \begin{cases} 1 & \text{if maximum} \\ 0 & \text{if not maximum} \end{cases} \quad (3)$$

where, p_j, p_k and p_m represent the neighborhood pixels in a row or column. Note that p_k is removed if it represents the center pixel. In comparison to conventional LBP, the proposed extended *hvnLBP* operator captures more discriminative contrast information and can achieve better retinal vein representation. The feature extracted by *hvnLBP* are further processed by proposed DE.

3.2 Conventional DE

Storn and Price [17] proposed DE to deal with global optimization in continuous spaces. DE algorithm employs the scaling factor between two individuals, which is also called as mutation factor. DE algorithm starts its search with the random initialization of vectors and tries to improve them to further obtain optimal solution. In DE the population with Np vectors in g generations is denoted as $P = \{X_1, X_1, \dots, X_{np}\}$ where, $X_i = (X_{i,a}, \dots, X_{i,D})$. Conventional DE consists of three important steps:

3.2.1 Mutation

In this step, three vectors from the population are selected randomly and the following mutation equation is applied:

$$V_i = X_{i_1} + F(X_{i_2} - X_{i_3}) \quad (4)$$

Where, $F \in [0, 2]$ it further controls the augmentation of the differential vector of $(X_{i_2} - X_{i_3})$. In DE, the F value plays very important role in controlling the exploration ability. Higher the F value higher the exploration ability and vice-versa.

3.2.2 Crossover

This step is applied to improve the diversity of the population by crossing the mutant and parent vector as follows:

$$U_{i,d} = \begin{cases} V_{i,d}, & \text{if } rand_d(0,1) \leq C_r \text{ or } d_{rand} = d \\ x_{i,d}, & \text{otherwise} \end{cases} \quad (5)$$

Where d is the dimension, C_r is the cross rate parameter, and the trial vector U_i can be generated as given below

$$U_i = (U_{i,1}, \dots, U_{i,D}) \quad (6)$$

3.2.3 Selection

This is the final step in each iteration, where U_i or X_i vector is selected based on their fitness value. The best fitness value vector is selected and sent for next iteration until the end condition is met.

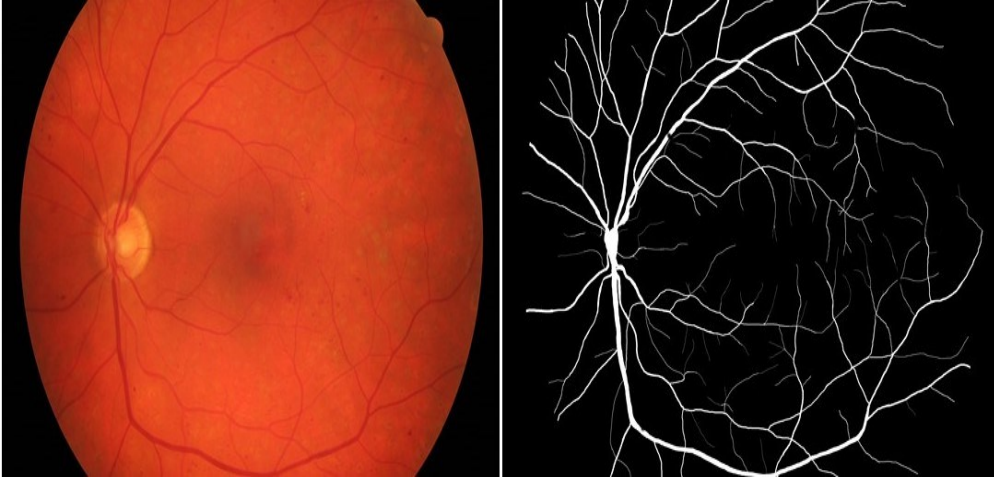


Figure 2: Segmentation results generated by proposed system for image from HRF dataset.

3.3 Proposed DE

The conventional Differential Evolution only employs one set of population to explore the search space [17]. The single set of population restricts the search in only one direction or one set of features. The

application of retinal blood vessel segmentation can lead to multiple clusters of features, which makes conventional DE less useful in this scenario.

Algorithm 1: The Pseudo Code of the Proposed DE Variant

Step-1 Initialize three sets of populations.

Step-2 Evaluate the fitness value for each population using the Equation 4. With separate criteria for each population.

Step-3 Store the current version of population in Non-replaceable memory.

Step-4 While (satisfying termination criteria)

 Perform standard DE steps as follows:

 Mutation using Equation 4.

 Crossover using Equation 5 and 6.

 Perform selection.

Re-evaluate the fitness value for everyone in the current population.

If (iterations ≥ 30)

 Select best individual from each population and compare it with members from Non-replaceable memory.

 Select the three most co-relating members and add them to Micro population along with the three global bests.

 Run FA for 100 iterations using Micro population

 Evaluate fitness for everyone in micro population using fitness criteria of the thin veins.

 Swap global bests if the newly generated members have higher fitness value.

End If

 Re-evaluate the fitness value for everyone in all populations.

End While

Step-4 End

In this paper, we employ a multi-population DE to cluster the retinal veins in three categories. First initializing number of populations with the same size of 30 members. Each population has its own fitness criteria i.e. the populations will look for thick blood vessels pixels, thin blood vessels pixels and non-blood vessel pixels. However, it simply means that three DE's will run in parallel to generate three sets of features.

In order to further diversify the populations and reduce the risk of premature convergence, we employ mGA's diversity maintenance strategy of non-replaceable memory [16]. During the first iteration we store all three populations in one set of non-replaceable memory. These stored members are further used to aid the micro population generation. After the first iteration we apply DE on all three populations and when the system reaches 30 iterations (selected based on experiments) a set of combined micro population will be created. This micro population will consist of 6 member including global best member from each population and three most correlating members from the non-replaceable memory. A FA with three mutation strategies will be applied to the micro population, which will generate new offspring based on thin vein fitness criteria over. If the newly generated members are better than the previous global bests then they will be replaced. In this version of FA we have employed gaussian mutation [16], Cauchy mutation [16] and levys flight mutations [16]. This allows the algorithm to find the best candidates to search the thin veins, as it is one of the challenging tasks. At the same time, it will improve the diversity and balance the global and local exploration. The overall structure of the proposed DE is illustrated in Algorithm 1. The fitness function used to evaluate each individual is given as follows:

$$F(x) = w_a * acc_x + w_f * (number_feature_x)^{-1} \quad (7)$$

where w_a and w_f are two predefined constant weights for acc_x (classification accuracy) and $number_feature_x$ (the number of features), respectively. In this paper, $w_a=0.8$ and $w_f=0.2$, with $w_a>w_f$ to represent the fact that classification accuracy is more important than the number of selected features. The Figure 2 shows the output results generated using the proposed system. The classification accuracy will be evaluated differently for each population.

Diverse classifiers have been employed to further identify vein and non-vein categories. The selected classifiers are popular in image analysis and have proved to show impressive performance as in our previous works [16] and [18]. NN, SVM, and the SVM-based and NN-based ensembles with SVM and NN as base classifiers respectively carry out

the vessel and non-vessel classification. The input layer for NN is assigned to a number of features extracted from the proposed model. The NN classifier contains a secret layer along with an output layer with 2 nodes denoting vessel or non-vessel. Furthermore, the grid-search mechanism is availed to generate the most favorable parameter settings for the SVM classifier with the aim of achieving optimal performance. The most favorable settings generated for every single model NN and SVM previously described are also applied to the settings of each base classifier within each ensemble. Both ensembles utilize three base classifiers and a weighted majority voting collaboration method to generate the final categorization. Overall, the NN and SVM-based ensembles achieve the best accuracy when subjected to the images from the databases used as described in the next section.

4. Evaluation

We have proposed an automatic retinal blood vessel segmentation system, which segments blood vessels from fundus image and outperforms most of the existing methodologies. The proposed system is evaluated using three datasets i.e. DRIVE [9], STARE [19], and HRF [20]. The STARE (STructured Analysis of the Retina) Project was conceived and initiated in 1975 by Michael Goldbaum, M.D., at the University of California, San Diego, USA. The STARE database has a set of around 400 raw retinal images. The DRIVE (Digital Retinal Images for Vessel Extraction) database were obtained from a diabetic retinopathy screening program in the Netherlands. The screening population consisted of 400 diabetic subjects between 25-90 years of age. Forty photographs have been randomly selected, 33 do not show any sign of diabetic retinopathy and 7 show signs of mild early diabetic retinopathy. The set of 40 images has been divided into a training and a test set, both containing 20 images. The HRF (High-Resolution Fundus) dataset has 15 retinal images of healthy patients, 15 images of patients with diabetic retinopathy and 15 images of glaucomatous patients which is gathered through a collaborative research group in Germany.

The proposed system is implemented from scratch using C++ and OpenCV library under Ubuntu operating system. The learning algorithms such as NN, SVM, NN- and SVM-based ensemble are imported from OpenCV and LibSVM library. The ground truth of the matching image is used to evaluate the performance of the proposed methodology on segmenting vessels from a fundus image. In order to measure the performance of the proposed system, we use accuracy, sensitivity, and specificity value. To calculate the accuracy, sensitivity, and specificity we have to consider four measures i.e., true positives, false positives, false negatives and true negatives. The correctly categorized vessel pixels as vessels are denoted as true positive (TP) and correctly categorized non-vessel pixels as non-vessels are denoted as true negative (TN). Whereas, wrongly categorized non-vessels pixels as vessels are denoted as false positive (FP) and wrongly categorized vessels pixels as non-vessels are denoted as false negative (FN). The equations used to calculate accuracy, sensitivity, and specificity value are as follows:

$$Accuracy = (TP + TN)/(TP + TN + FP + FN) \quad (8)$$

$$Sensitivity = TP/(TP + FN) \quad (9)$$

$$Specificity = TN/(TN + FP) \quad (10)$$

In order to evaluate the performance of the proposed DE, it is compared with the existing state-of-the-art evolutionary algorithms. The selected evolutionary algorithms include, GA [21], DE [17], FA [22], PSO [23], Moth Flame Optimization (MFO) [24], and Whale Optimization algorithm (WOA) [25]. Moreover, this paper presents three set of results containing results using NN, SVM, ensemble NN and ensemble NN.

The first set of results presents the results using DRIVE dataset for training and testing. This set is illustrated in Table 1 to 4 and each table shows the average accuracy, sensitivity and specificity of all the images in DRIVE datasets over the 30 runs. The results obtained clearly shows that the proposed DE outperforms the selected evolutionary algorithms while WOA being very close and second best. Overall the Table 4 shows

that SVM-based ensemble classifier can obtain best results for all the selected algorithms with proposed DE achieving the best results.

Table I Performance of proposed system using NN classifier on DRIVE dataset

	Accuracy	Sensitivity	Specificity
GA	91.1	79.3	90.5
DE	92.5	81.7	91.3
FA	92.0	82.4	93.6
PSO	90.4	80.5	91.7
MFO	93.8	83.2	94.0
WOA	95.1	84.3	94.8
Proposed DE	95.5	85.1	96.3

Table II Performance of proposed system using SVM classifier on DRIVE dataset

	Accuracy	Sensitivity	Specificity
GA	91.5	80.0	89.7
DE	91.8	81.6	92.4
FA	93.2	83.0	92.9
PSO	92.6	82.8	93.0
MFO	94.4	85.5	95.1
WOA	96.0	86.6	95.7
Proposed DE	96.0	87.0	96.2

Table III Performance of proposed system using Ensemble NN classifier on DRIVE dataset

	Accuracy	Sensitivity	Specificity
GA	91.5	80.0	91.5
DE	92.2	81.9	94.3
FA	94.8	84.0	93.7
PSO	93.5	84.3	94.8
MFO	95.6	86.4	95.1
WOA	97.4	86.9	96.4
Proposed DE	96.7	88.1	97.7

Table IV Performance of proposed system using Ensemble SVM classifier on DRIVE dataset

	Accuracy	Sensitivity	Specificity
GA	93.2	80.0	91.0
DE	93.6	82.6	93.9
FA	94.4	83.8	93.6
PSO	93.0	84.6	94.2
MFO	96.4	85.8	96.1
WOA	96.4	86.6	95.9
Proposed DE	97.9	87.8	96.2

Table V Performance of proposed system using NN classifier on STARE dataset

	Accuracy	Sensitivity	Specificity
GA	91.4	78.9	87.0
DE	90.6	79.6	87.1
FA	91.8	80.4	88.2
PSO	91.4	80.8	87.1
MFO	91.9	82.4	90.0
WOA	92.9	83.3	91.8
Proposed DE	94.0	84.9	92.7

Table VI Performance of proposed system using SVM classifier on STARE dataset

	Accuracy	Sensitivity	Specificity
GA	90.8	78.1	86.3
DE	90.2	79.8	86.9
FA	91.4	80.9	88.0
PSO	91.1	81.3	87.3
MFO	91.4	82.3	90.2
WOA	92.8	82.9	92.1
Proposed DE	93.1	85.2	93.0

The second set of results presents the results using STARE dataset for training and testing. This set is illustrated in Table 5 to 8 and each table shows the average accuracy, sensitivity and specificity of all the images in STARE datasets over the 30 runs. The results obtained clearly shows that the proposed DE outperforms the selected evolutionary algorithms. The performance results obtained by WOA are significantly lower than the proposed DE compared to results obtained in First set. Overall the Table 8 shows that SVM-based ensemble classifier can obtain best

results for all the selected algorithms with proposed DE achieving 99.2% average accuracy.

Table VII Performance of proposed system using Ensemble NN classifier on STARE dataset

	Accuracy	Sensitivity	Specificity
GA	92.5	79.0	86.6
DE	90.6	80.7	88.2
FA	93.6	82.7	90.1
PSO	92.0	82.1	89.1
MFO	92.5	82.9	91.8
WOA	95.6	85.5	92.6
Proposed DE	96.0	84.8	93.0

Table VIII Performance of proposed system using Ensemble SVM classifier on STARE dataset

	Accuracy	Sensitivity	Specificity
GA	90.6	78.7	86.3
DE	91.0	81.1	89.1
FA	92.7	81.9	89.4
PSO	90.9	82.3	88.3
MFO	93.1	83.5	90.6
WOA	97.5	85.3	93.8
Proposed DE	99.2	86.1	96.4

Table IX Performance of proposed system using NN classifier on HRF dataset

	Accuracy	Sensitivity	Specificity
GA	86.6	75.9	81.9
DE	86.5	76.2	82.8
FA	88.4	77.5	83.6
PSO	88.6	76.3	83.8
MFO	89.2	80.4	85.4
WOA	90.3	80.0	86.5
Proposed DE	91.6	81.1	88.4

The third set of results presents the results using HRF dataset for training and testing. This set is illustrated in Table 9 to 12 and each table shows the average accuracy, sensitivity and specificity of all the images in HRF datasets over the 30 runs. The results obtained clearly shows that the proposed DE outperforms the selected evolutionary algorithms while WOA being the second best. The performance results obtained by WOA

are significantly lower than the proposed DE compared to results obtained in First set. Overall the Table 4 shows that SVM-based ensemble classifier can obtain best results for all the selected algorithms with proposed DE achieving 98.3% average accuracy.

Table X Performance of proposed system using SVM classifier on HRF dataset

	Accuracy	Sensitivity	Specificity
GA	86.9	75.2	81.5
DE	86.9	76.3	82.5
FA	89.0	78.0	83.4
PSO	88.6	76.3	83.5
MFO	89.7	80.3	85.8
WOA	90.9	80.6	86.3
Proposed DE	91.0	81.2	88.6

TABLE XI Performance of proposed system using Ensemble NN classifier on HRF dataset

	Accuracy	Sensitivity	Specificity
GA	87.0	76.0	83.6
DE	87.4	76.3	84.6
FA	89.7	78.1	83.2
PSO	88.5	78.8	85.1
MFO	92.2	83.6	89.9
WOA	93.3	84.8	90.8
Proposed DE	97.2	86.1	93.8

Table XII Performance of proposed system using Ensemble SVM classifier on HRF dataset

	Accuracy	Sensitivity	Specificity
GA	88.3	75.5	83.4
DE	88.5	76.5	84.0
FA	88.1	78.1	84.0
PSO	90.0	77.9	84.4
MFO	94.5	84.7	86.6
WOA	95.4	85.1	91.4
Proposed DE	98.3	87.0	94.9

A comparison of the proposed DE based system using SVM-based ensemble classifier with other existing systems is illustrated in Table V. The proposed system is able to show better performance than other methodologies when evaluated with three publicly available datasets.

Table XIII Performance comparison with existing methodologies

Dataset	Methodology	Accuracy	Sensitivity	Specificity
DRIVE	Proposed work	97.9	87.8	96.2
	Wang et al. [5]	97.7	81.7	97.3
	Moghimirad et al. [26]	96.6	78.5	99.4
	GeethaRamani et al. [27]	95.4	70.8	97.8
	Imani et al. [28]	95.2	75.2	97.5
	Franklin and Rajan [29]	95.0	68.7	98.2
	Roychowdhury et al. [30]	95.2	72.5	98.3
	Liu et al. [31]	94.7	73.5	97.7
STARE	Proposed work	99.2	86.1	96.4
	Wang et al. [5]	98.1	81.0	97.9
	Moghimirad et al. [26]	97.6	81.3	99.1
	Imani et al. [28]	95.9	75.0	97.5
	Annunziata, et al. [32]	95.6	71.3	98.4
	Roychowdhury et al. [30]	95.2	77.2	97.3
	Liu et al. [31]	95.7	76.3	97.1
HRF	Proposed work	98.3	87.0	94.9
	Christodoulidis et al. [33]	94.8	85.1	95.8
	Cheng et al. [34]	96.1	70.4	98.6
	Annunziata, et al. [32]	95.8	71.3	98.4
	Lázár et al. [35]	95.3	71.0	98.3
	Odstrcilik et al. [20]	94.9	77.4	96.7

Table XIII shows that the proposed system outperforms specifically the works of Wang et al., Moghimirad et al., GeethaRamani et al., Imani et al., Franklin et al., Cheng et al., and others when evaluated with DRIVE, STARE and HRF datasets. For the DRIVE dataset the new proposed algorithm had achieved 97.9% accuracy, for STARE dataset 99.2%

accuracy and for HRF dataset 98.3% accuracy, giving an average accuracy across three datasets to be 98.4%, along with 86.9% average sensitivity and 95.8% average specificity. The above results show that the proposed system can accurately segment the blood vessels from the retinal fundus images. The further analysis of segmented vessels using the proposed system can lead to automatic disease diagnosis like diabetic retinopathy, artery and vein occlusion, hypertensive retinopathy. Thus, the proposed system can benefit ophthalmologists in the screening of retinal diseases more efficiently.

5. Discussion and Conclusion

In this paper, we have proposed an automatic retinal blood vessel segmentation system, which segments blood vessels from fundus image while outperforming the other state-of-the-art systems. The overall system show significant improvement in the segmentation and classification for efficient retinal image analysis. The proposed system uses a mFA embedded multi-population differential evolution (DE) algorithm in order to carry out automatic retinal blood vessel segmentation on retinal images. Multiple classifiers are used to identify whether the retinal blood vessel images are healthy or unhealthy (i.e. with retinal disease). The proposed system is evaluated using three publicly available datasets such as DRIVE, STARE and HRF. Upon evaluation, the proposed system is able to achieve a high average accuracy of 98.4% on three datasets, which is on par with most of the systems reported in the literature. Due to its noticeable accuracy, this system could benefit the ophthalmologists for retinal image analysis. It can further help in diagnosing the retinal diseases at an earlier stage, which can lead to successful treatment of the eye patients. As far as we know, no one has attempted a differential evolution variant for retinal image analysis and diagnosis and hence the work is novel.

References

- [1] E. Emary, H. M. Zawbaa, A.E. Hassanien, G. Schaefer and A. T. Azar, "Retinal blood vessel segmentation using bee colony optimisation and pattern search," 2014 International Joint Conference on Neural Networks (IJCNN), Beijing, pp. 1001-1006, 2014.
- [2] G. Hassan, A. E. Hassanien, N. El-bendary and A. Fahmy, "Blood vessel segmentation approach for extracting the vasculature on retinal fundus images using Particle Swarm Optimization," 2015 11th International Computer Engineering Conference (ICENCO), Cairo, pp. 290-296, 2015.
- [3] K. S. Sreejini, V. K. and Govindan, "Improved multiscale matched filter for retinal vessel segmentation using PSO algorithm," Egyptian Informatics Journal, 16(3), pp.253-260, 2015.
- [4] R. Arnay, F. Fumero and J. Sigut, "Ant Colony Optimization-based method for optic cup segmentation in retinal images," Applied Soft Computing, 52, pp. 409-417, 2017.
- [5] S. Wang, Y. Yin, G. Cao, B. Wei, Y. Zheng, and G. Yang, "Hierarchical retinal blood vessel segmentation based on feature and ensemble learning," Neurocomputing, 149(B), pp. 708-717, 2015.
- [6] S. Morales, K. Engan, V. Naranjo, and A. Colomer, "Retinal Disease Screening Through Local Binary Patterns," IEEE Journal of Biomedical and Health Informatics 21(1):184-192, 2017
- [7] N. Hatami and M. Goldbaum, "Automatic Identification of Retinal Arteries and Veins in Fundus Images using Local Binary Patterns," Investigative Ophthalmology and Visual Science, 55 (5):232, 2016.
- [8] M. M. Fraz, P. Remagnino, A.Hoppe, B. Uyyanonvara, A.R.Rudnicka, C.G.Owen, S.A. Barman, "Blood vessel segmentation methodologies in retinal images—a survey," Comput Methods Programs Biomed 108(1):407-33, 2012
- [9] J. Staal, M. D. Abramoff, M. Niemeijer, M. A. Viergever and B.V. Ginneken, "Ridge-based vessel segmentation in color images of the retina," IEEE Trans Med Imaging 23(4):501–9, 2004.
- [10] D. Marin, A. Aquino, M. E. Gegundez-Arias and J. M. Bravo, "A new supervised method for blood vessel segmentation in retinal images by using gray-level and moment invariants-based features," IEEE Trans Med Imaging 30(1):146-58, 2011.

- [11] X. You, Q. Peng, Y. Yuan, Y-M. Cheung, and J. Lei, "Segmentation of retinal blood vessels using the radial projection and semi-supervised approach," *Pattern Recognition* 44:2314–24, 2011.
- [12] A. Budai, R. Bock, A. Maier, J. Hornegger and G. Michelson, "Robust Vessel Segmentation in Fundus Images," *International Journal of Biomedical Imaging*, 11 pages, 2013.
- [13] J. Hannink, R. Duits and E. Bekkers, "Crossing-Preserving Multi-scale Vesselness", In: "Medical Image Computing and Computer-Assisted Intervention," *International Conference on Medical Image Computing and Computer-Assisted Intervention: Springer*, 8674, 2014.
- [14] T. Chakraborti, D. K. Jha, A S Chowdhury and X Jiang, "A Self-Adaptive Matched Filter for Retinal Blood Vessel Detection," *Machine Vision and Applications. Berlin Heidelberg: Springer Verlag*. 26:55, 2015.
- [15] T. Ojala, M. Pietikainen, and D. Harwood, "A comparative study of texture measures with classification based on featured distribution," *Pattern Recognit.*, vol. 29, no. 1, pp. 51–59, 1996.
- [16] K. Mistry, L. Zhang, S. C. Neoh, C. P. Lim, and B. Fielding, "A micro-GA Embedded PSO Feature Selection Approach to Intelligent Facial Emotion Recognition," *IEEE Transactions on Cybernetics*, 47(6), pp.1496 - 1509, 2016.
- [17] R. Storn and K. Price, "Journal of Global Optimization" 11: 341, 1997. [29] N. Strisciuglio, G. Azzopardi, M. Vento and N. Petkov, "Multiscale blood vessel delineation using B-cosfire filters," In: *International Conference on Computer Analysis of Images and Patterns. Springer*, pp.300–312, 2015.
- [18] S. C. Neoh, L. Zhang, K. Mistry, M. A. Hossain, C. P. Lim, N. Aslam, and P. Kinghorn, "Intelligent Facial Emotion Recognition Using a Layered Encoding Cascade Optimization Model," *Appl Soft Comput. Volume 34*, 72–93, 2015.
- [19] A.D. Hoover, V. Kouznetsova and M. Goldbaum, "Locating blood vessels in retinal images by piece-wise threshold probing of a matched filter response," *IEEE Trans. Med. Imaging* 19, 203–210, 2000.
- [20] J. Odstrcilik, R. Kolar, A. Budai, J. Hornegger, J. Jan, J. Gazarek, T. Kubena, P. Cernosek, O. Svoboda and E. Angelopoulou, "Retinal vessel segmentation by improved matched filtering: evaluation on a new high-resolution fundus image database," *IET Image Process.* 7, 373–383, 2013.
- [21] J.H. Holland, "Genetic Algorithms". In *Sci. Am.* 267, 66-72, 1992.

- [22] X.S. Yang. 2010. "Firefly algorithm, Levy's flight and global optimization", *Research and Development in intelligent systems* 26 (2010) 209-218.
- [23] R.C. Eberhart, J. Kennedy, "A new optimizer using particle swarm theory", In: *Proceedings of the Sixth International Symposium on Micro Machine and Human Science*, pp. 39-43, 1995.
- [24] S. Mirjalili, "Moth-Flame optimization algorithm: A novel nature-inspired heuristic paradigm", *Knowl. Based Syst.* 89 (2015) 228-249.
- [25] S. Mirjalili, A. Lewis, "The whale optimization algorithm", *Adv. Eng. Softw.* 95 (2016) 51-67.
- [26] E. Moghimirad, S. H. Rezaatofghi, and H. Soltanian-Zadeh, "Retinal vessel segmentation using a multi-scale medialness function," *Comput. Biol. Med.* 42:50-60, 2012.
- [27] R. GeethaRamani, L. Balasubramanian, "Retinal blood vessel segmentation employing image processing and data mining techniques for computerized retinal image analysis," *Biocybernetics and Biomedical Engineering*, 36(1):102-118, 2016.
- [28] E. Imani, M. Javidi, and H. Pourreza, "Improvement of retinal blood vessel detection using morphological component analysis," *Comput. Methods Progr. Biomed.* 118:263-279, 2015.
- [29] S. W. Franklin and E. Rajan, "Computerized screening of diabetic retinopathy employing blood vessel segmentation in retinal images," *Biocybern Biomed Eng* 34:117-24, 2014.
- [30] S. Roychowdhury, D.D. Koozekanani, and K. K. Parhi, "Blood vessel segmentation of fundus images by major vessel extraction and subimage classification," *IEEE J. Biomed. Health Inf.* 19, 1118-1128, 2015.
- [31] X. Liu, Z. Zeng and X. Wang, "Vessel segmentation in retinal images with a multiple kernel learning based method," In: *2014 International Joint Conference on Neural Networks (IJCNN)*. IEEE, pp. 507-511, 2014.
- [32] R. Annunziata, A. Garzelli, L. Ballerini, A. Mecocci, and E. Trucco, "Leveraging Multiscale Hessian-Based Enhancement with a Novel Exudate inpainting Technique for Retinal Vessel Segmentation," *IEEE Journal Biomed Health Inform.* 20(4):1129-38, 2015.
- [33] A. Christodoulidis, T. Hurtut, H. B. Tahar, and F. Cheriet, "A multi-scale tensor voting approach for small retinal vessel segmentation in high-resolution fundus images," *Comput. Med. Imaging Graph.* 52:28-43, 2016.

- [34] E. Cheng, L. Du, Y. Wu, Y. J. Zhu, V Megalooikonomou, and H. Ling, "Discriminative vessel segmentation in retinal images by fusing context-aware hybrid features," *Mach. Vis. Appl.* 25:1779–1792, 2014.
- [35] I. La'za'r and A. Hajdu, "Segmentation of retinal vessels by means of directional response vector similarity and region growing," *Comput. Biol. Med.* 66, 209–221, 2015.